

Solids circulation rate and static bed height in a riser of a circulating fluidized bed

Daebum Cho^{*}, Jeong-Hoo Choi^{**†}, Muhammad Shahzad Khurram^{**}, Sung-Ho Jo^{***},
Ho-Jung Ryu^{***}, Young Cheol Park^{***}, and Chang-Keun Yi^{***}

^{*}Ansan Technical High School, 51 Ansongonggo-ro, Sangnok-gu, Ansan-si, Gyeonggi 426-829, Korea

^{**}Department of Chemical Engineering, Konkuk University, 1 Hwayang-dong, Gwangjin-gu, Seoul 143-701, Korea

^{***}Korea Institute of Energy Research, 71-2, Jang-dong, Yuseong-gu, Daejeon 305-343, Korea

(Received 30 April 2014 • accepted 22 July 2014)

Abstract—Solids circulation rate and static bed height in the riser of a circulating fluidized bed (CFB) process, which consisted of a riser and two bubbling-beds, were investigated and discussed at ambient temperature and pressure. Three kinds of powder (FCC catalyst, glass bead, plastic powder) were used as bed materials. The static bed height in the riser increased with the solids circulation rate. However, it decreased with an increase of gas velocity. The effect of gas velocity diminished as the gas velocity increased. The riser static bed height could be used to estimate the solids circulation rate in reasonable accuracy. A correlation on static bed height in the riser, relating to the solids circulation rate, was proposed for the present experimental ranges.

Keywords: Solids Circulation Rate, Static Bed Height, Pressure Drop, Solids Inventory, Solids Holdup, Riser, Circulating Fluidized Bed

INTRODUCTION

The dual gas fluidized-bed system of a fast bed riser and a bubbling bed is used for a reactor-regenerator process such as the process capturing CO₂ from flue gas [1] and the desulfurization process for coal gas [2]. The process consists of a riser type adsorption column and a bubbling-bed regenerator. In the adsorption column, the solid particles controlled in flow rate by a mechanical valve such as a rotary valve or a slide gate adsorb target gas components. Particles are sent to the regenerator to release the adsorbate and return to the adsorption column. This process considers the solids circulation rate and the solids inventory in each reactor as essential factors affecting process performance. The solids flow rate affects solids holdup, mass and energy balances in the riser. The solids holdup relates to the size of the fan that supplies fluidizing gas to the riser since the solids holdup is one of main factors contributing the pressure drop in the riser. The solids holdup in the riser also should provide proper mean residence times of solid and gas phases for reaction.

However, there hardly exist proper methods to measure the solids circulation rate for the CFB system. Most measuring methods have been improper in simplicity and robustness to apply for industrial systems [3]. There has not been much attention given to providing a tool to predict the solids circulation rate generally in the riser. Thus, Martin and Ommen [3] mentioned that correlation between pressure drop (or solids holdup) of a riser section and the solids circulation rate remains as one of the most common methods used in industry for the online estimation of the solids mass

flux. The correlation can be set up between the average solids holdup and the solids circulation rate in the riser.

The solids holdup in the riser is an integration of the axial solids holdup profile along the entire riser height that considers the dense region in the bottom, the dilute region in the top, and transition region between dense and dilute region as summarized by Bai and Kato [4]. The axial solids holdup profile divided into three types depending on existence of dilute region only, dilute and transition regions, and all three regions (typical S-profile) as solids flow rate increased for a certain gas velocity. It is represented by empirical correlations [5-7] or comprehensive models, the so-called pressure balance models [8]. Empirical correlations limited application ranges as their own experimental conditions, but were not in good agreement even with their own data. The pressure balance model summarized by Lei and Horio [8] was very complex in use but established systematic understandings on this system. It needs the pressure balance over the whole system of the CFB including the riser and the external loop which connects with each other at the top and the bottom, respectively. As examples, the inflection point of the model of Li and Kwauk [9] and dense region height of the model of Lei and Horio [8] for the axial solids holdup profile of the riser cannot be calculated without the pressure balance since the head of the gas-solids mixture in the riser is attributed to the counter balance of the pressure head of the external loop in the model. The external loop consists of a cyclone collector and a return leg at least, often including a reservoir and/or a valve additionally for the dual fluidized bed system [1,2,10]. There can be various types of valves in use such as a rotary valve [5], a slide gate [1,2], a loopseal and an L-valve. Pressure drop in the cyclone and the reservoir is rather simple to estimate as an approximation. But it is still very difficult to predict the valve pressure drop depending on type and geometry of valve, solids circulation rate, and aeration rate. In the mean-

[†]To whom correspondence should be addressed.

E-mail: choijhoo@konkuk.ac.kr

Copyright by The Korean Institute of Chemical Engineers.

time, conditions of riser bottom and return leg also affect the pressure balance. The exit of the valve or the downward return leg is often connected to a transition or dilute region of the riser, and most of the upper part except the small lower part of the return entry is empty like gravity feeding without aeration [1,2]. Then the valve almost consumes pressure head of the external loop, the pressure balance loop set up regardless of the solids holdup of dense region in the bottom of the riser, and the axial solids holdup profile including the inflection point or dense region height can hardly be determined in the riser. Kato et al. [6] and Rao et al. [7] proposed correlations on height of inflection point. But their correlations cannot fulfill the need of above models completely since they do not cover the imaginary inflection point located below the distributor level. Thus, the pressure balance model is still too complex and not totally available for actual use. Kunii and Levenspiel [11] proposed a model to relate the riser solid holdup profile with the solids circulation rate without the use of a pressure balance. However, their model was too simple to represent the dilute region and transition region properly. Sum of the height of both regions is only subjected to decay constant that describes the solids holdup profile decreasing from the top end of the dense region to the gas exit of the riser. The decay constant and solids holdup of the dense region was only a function of gas velocity. With their model for a high riser, the height of the dilute region is underestimated, but inversely the height of the dense region overestimated as the rest of the riser height. Bai and Kato [4] summarized that previous models and correlations on solids holdup for dense and dilute regions indicated relative deviations $>68\%$ at the dense region and $>50\%$ at the dilute region from measured data, respectively. They made good improvement with new correlations on them with relative errors ranging from 14.4% to 19.7%. However, solids holdup of transition and dense regions, determined by applying decay constant [8] and inflection point (or dense region height) [6,7], respectively, will have to add further error (10% to 30% at least) to total solids holdup. Chan et al. [12] proposed correlations for average solids holdup together with a quite different flow regime map from previous ones in type of axial solids holdup profile. Zone IV in their regime map had an initial acceleration zone (IAZ) in the bottom when a bubbling/turbulent fluidized bed (S-profile) was formed. Both exponential profile and S-profile accordingly occurred together in the riser. In addition, the typical S-profile was a transition from dilute flow (DF) to fully developed dense suspension upflow (DSU). As a result, existing correlations and models on axial solids holdup profile in the riser are very complicated but not established well enough to use for estimating the total solids holdup. It might be better to develop new direct relationship between total solids holdup and solids flow rate in the riser.

The purpose of this study was to investigate the feasibility of a simple relationship between solids flow rate and pressure drop in the riser of a circulating fluidized bed as a method to determine them with information only on riser conditions.

EXPERIMENT

The experimental set-up (Fig. 1) consisted of a riser (0.025 m-i.d., 3.0 m-high), cyclones, a loopseal, two bubbling fluidized-beds

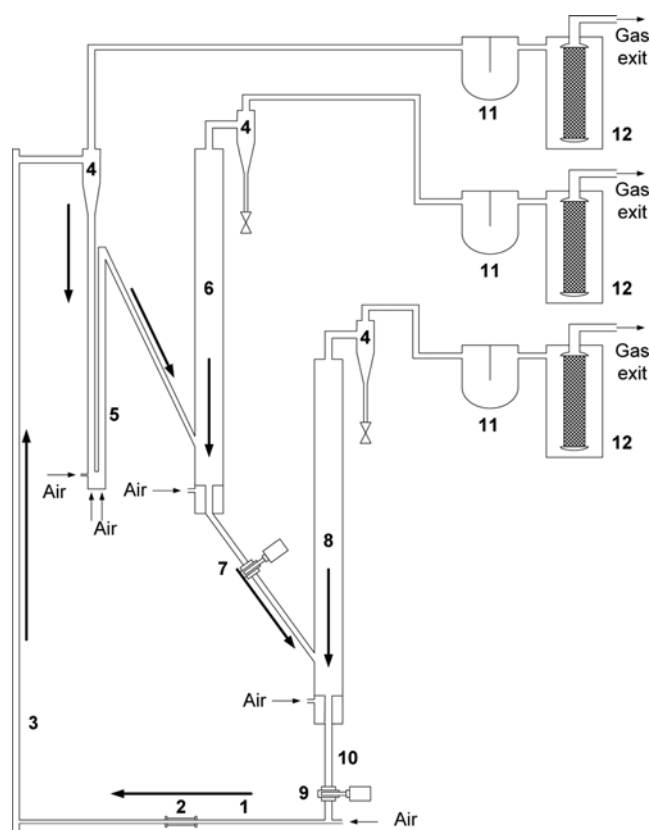


Fig. 1. Experimental setup.

- | | |
|-------------------------------|-------------------------------|
| 1. Horizontal pipe | 7. Slide valve (1) |
| 2. Sight glass | 8. Bubbling fluidized-bed (2) |
| 3. Riser | 9. Slide valve (2) |
| 4. Cyclone | 10. Standpipe |
| 5. Loopseal | 11. Settling chamber |
| 6. Bubbling fluidized-bed (1) | 12. Bag filter |

(0.1 m-i.d., 1.2 m-high) stepwise, and two stainless steel slide valves - one between two bubbling fluidized-beds (1) and (2), and another below the bubbling fluidized-bed (2).

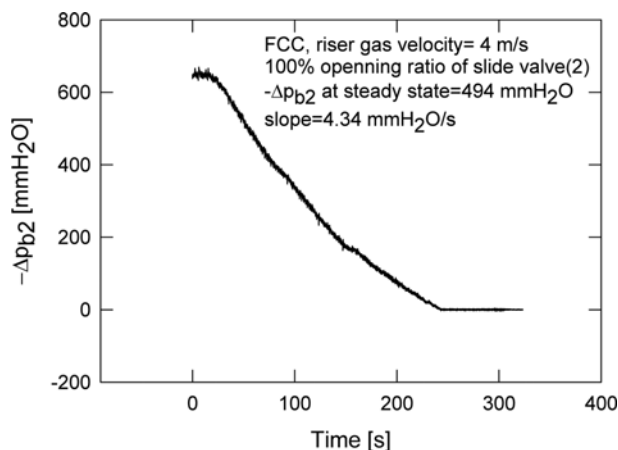
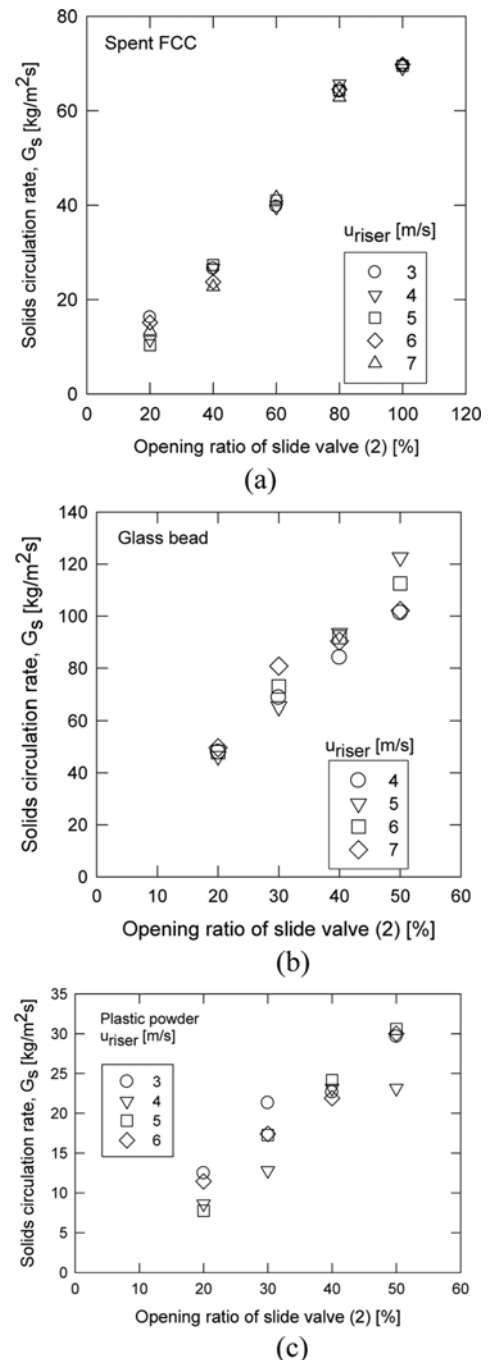
The feed gas to the riser contained particles from the lower bubbling fluidized bed (2) through a standpipe. The particles were dropped into the conveying gas stream at the T-junction below the slide valve (2). The flow rate of solids was controlled by changing the opening of the slide valve (2) placed in the standpipe from the bottom of the lower bubbling bed (2). The entrained particles were separated from gas in a cyclone separator and sent to the upper bubbling fluidized bed (1). The bottom of the upper bubbling bed (1) and freeboard of the lower bubbling bed (2) were connected with a standpipe via a slide valve (1). The slide valve (1) was used to cut the solids flow between two bubbling beds (1) and (2). Both bubbling beds were fluidized as 0.023-0.171 m/s, a little greater than the minimum fluidization condition. Each bubbling bed had a cyclone to capture particles entrained by exit gas. But the amount of entrained particles was small enough to neglect without return. Each solids holdup in the riser and bubbling beds was estimated from the differential pressure across the bed. Table 1 summarizes properties of particles used as bed materials. Three kinds of solid particles were used as bed materials.

Table 1. Particle properties

| Properties | Spent FCC | Glass bead | Plastic powder |
|--|-----------|------------|----------------|
| Apparent density [kg/m ³] | 1588 | 2486 | 918 |
| Bulk density [kg/m ³] | 735 | 1451 | 415 |
| Specific surface mean diameter [mm] [11] | 0.0799 | 0.0926 | 0.348 |
| Minimum fluidizing velocity [m/s] | 0.00382 | 0.0114 | 0.0849 |
| Transport velocity [m/s] [13] | 1.56 | 2.10 | 2.48 |
| Terminal velocity [m/s] [11] | 0.304 | 0.638 | 1.407 |
| Geldart's classification [14] | AB | B | B |

Gas velocity and solid circulation rate in the riser were considered as independent variables for each bed material. The riser gas flow rate was controlled by a mass flow controller. To estimate the solids circulation rate in the steady state solids circulation test, we ran a transient transport test of solids from the lower bubbling bed (2) to the upper bubbling fluidized bed (1) through the slide valve (2), the riser and the cyclone. The two bubbling beds were fluidized and the slide valve (1) between two bubbling beds (1) and (2) cut the solids flow during the test. The solids circulation rate was supposed to depend on the lower bubbling bed height, the opening of the slide valve (2) and the riser gas velocity. The solids flow rate was measured at the opening ratio of slide valve (2) and the riser gas velocity of steady state experimental conditions.

Initially, the lower bubbling bed (2) was charged with solids, the upper bubbling bed (1) was empty, and gas velocities for the riser, bubbling beds (1) and (2) were set. We started measuring the transient change of differential pressure in the bubbling bed (2) as we opened the slide valve (2) quickly to an opening ratio. Particles were conveyed to the bubbling bed (1), and the slope of transient differential bed pressure in bubbling bed (2) changed as bed mass decreased. In the run we got the transient trend of bed mass from the differential pressure change across the lower bubbling bed (2). Fig. 2 shows a sample trend. The instantaneous solids flow rate at a height of the lower bubbling bed (2) was determined by the slope of the transient bed mass trend. We calculated the solids flow rate for a bed differential pressure drop of the bubbling bed (2) from the transient change of differential pressure drop of the bed. There-

**Fig. 2. Transient loss of bed mass in bubbling fluidized bed (2).****Fig. 3. Solids circulation rate in the riser at steady state conditions.**

fore, the solids flux (G_s) in the riser at a certain differential pressure of the bubbling bed (2) ($-\Delta p_{b2}$) was calculated as

$$G_s = \left(\frac{d(-\Delta p_{b2}/g)}{dt} \right)_{at a(-\Delta p_{b2})} \frac{A_{b2}}{A_r} \quad (1)$$

A_{b2} and A_r are cross-sectional areas of bubbling bed (2) and riser, respectively. Fig. 3 indicates the solids circulation rate in steady state solids circulation tests for particles. The solids circulation rate increased as the opening ratio of slide valve (2) increased nearly proportionally, but the effect of riser gas velocity was arbitrary.

RESULTS AND DISCUSSION

Figs. 4 shows typical axial solids holdup profiles in the riser for three kinds of particles (FCC, glass bead, plastic). Since the effect of solids flux rather than wall friction on the axial pressure loss seemed dominant and the solids flux of this study was $<199 \text{ kg/m}^2\text{s}$ [15, 16], effects of particle acceleration and wall friction on the axial pressure loss were considered negligible in this study even though the riser diameter of this study 0.025 m was smaller than that of Arena et al. [15] 0.041 m. The average solids holdup (ε_p) in the section could be determined from an axial differential pressure gradient by Eq. (2).

$$(-\Delta p/\Delta h) = \varepsilon_p \rho_p g \quad (2)$$

The solids holdup decreased steeply in the lower dense region for all particles as height increased. It decreased due to particles being speeded up in this acceleration zone (AZ) [4]. It decreased slowly in the middle for FCC particles and plastic powder and then increased in the top section for all particles. The increasing trend of the top section seemed to be due to the abrupt gas exit and reflux of solids bouncing back against the ceiling [17]. The solids holdup in bottom and top sections increased with an increase of solids circulation rate or particle density as usual [4,17]. In case of plastic powder, a zone of constant solids holdup, which seemed a zone of fully accelerated particles, appeared in the middle of the riser (Fig. 4(d)) for some experimental conditions. However, we could rarely have the zone in present riser conditions and hardly use the solids holdup of this zone to calculate the solids circulation rate.

Modes of operation by Chan et al. [12] indicated that the present riser circulating FCC particles with $G_s < 27.3 \text{ kg/m}^2\text{s}$ fell in mode II for dilute flow (DF) with AZ in the bottom and $G_s > 62.8 \text{ kg/m}^2\text{s}$ in mode IV for core-annulus flow (CAF) with dense bubbling/turbulent fluidized bed (BTFB). The CAF with dense BTFB had the initial AZ (IAZ) in the bottom and the S-profile of axial solids holdup consecutively. The mode III for CAF with AZ in the bottom was

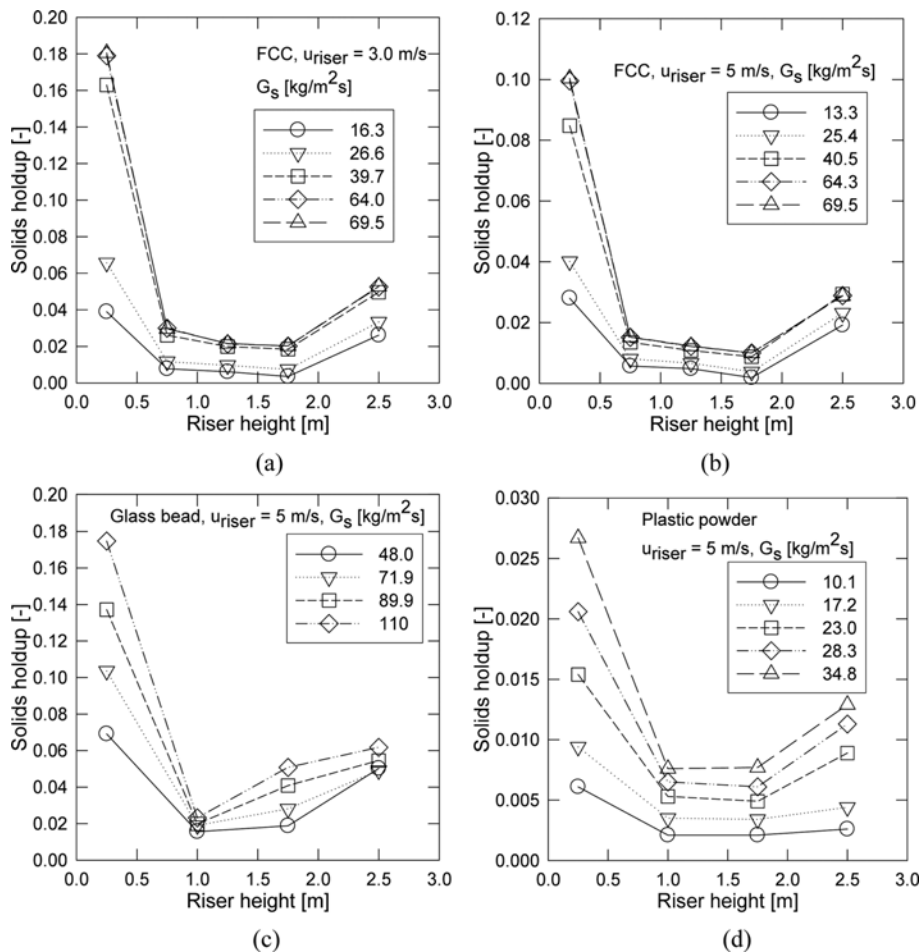


Fig. 4. Axial solids holdup profile in the riser (a), (b) FCC, (c) glass bead, (d) plastic powder.

expected between them in G_s . According to the correlation of Bai and Kato [4], the present G_s , except $64.0 \text{ kg/m}^2\text{s}$ and $69.5 \text{ kg/m}^2\text{s}$ for 3 m/s , was less than the saturation carrying capacity. Then the S-profile of axial solids holdup was expected only for those two conditions. Since solids holdup profiles measured for $G_s > 62.8 \text{ kg/}$

m^2s were similar for all gas velocities and modes of operation of Chan et al. [12] always had the AZ in the bottom, the model of Chan et al. [12] seemed to be better than that of Bai and Kato [4]. However, both models did not consider the exit effect on solids holdup.

Fig. 5 indicates effects of gas velocity and solids circulation rate on the static bed height in the riser for (a) FCC, (b) glass bead and (c) plastic powders. The static bed height was determined by Eq. (3) as the total bed height converted to minimum fluidizing condition.

$$h_s = \frac{(-\Delta p)_r}{\rho_{p,bulk} g} \quad (3)$$

The static bed height of FCC particles decreased in Fig. 5(a) as the gas velocity increased. The effect of gas velocity decreased as the gas velocity increased. However, the static bed height of solids increased as the solids circulation rate increased. The decreasing trend of solids static bed height by an increase of gas velocity slowed as the solids circulation rate decreased.

As gas velocity increases, the relative velocity between solid and gas increases, the drag force on the particle surface increases, the rising velocity of particle increases, then the solid holdup, i.e., static bed height of solids, decreases for a certain solids circulation rate [4]. The static bed height of solids increases due to the increase of solid holdup as the solids circulation rate increases. Time for fully accelerating the particles in the bottom of the riser increases as the solids circulation rate increases. It decreases as the gas velocity or the ratio of gas flow rate to solids flow rate increases. Therefore, the solids static bed height increased as the solids circulation rate increased, and effects of gas velocity and solids circulation rate decreased as the ratio of solids flow rate to gas flow rate decreased.

Effects of gas velocity and solids circulation rate on the static bed height in the riser for glass bead particles were found similar to those for FCC particles, as can be seen in Fig. 5(b). The solids circulation rate was greater than that of FCC particles for the same opening ratio of the slide valve because the bulk density of glass beads was greater than FCC particles. The static bed height of glass beads in the riser increased more proportionally with increasing the solids circulation rate than that of FCC particles. Effects of gas velocity and solids circulation rate on the static bed height of plastic powder in the riser were similar to those for FCC particles and glass beads but rather closer to those for glass beads, as can be seen in Fig. 5(c). It seemed to be attributed to the same Geldart classification B [14]. The static bed height of plastic powders in the riser decreased more linearly than those of FCC particles, and glass beads as the gas velocity increased.

Fig. 6 compares riser static bed heights for different types of particles. The static bed height of glass bead was smaller for similar gas velocities and solids circulation rates than FCC particles, because glass bead is heavier in apparent density and bigger. However, FCC particles (Fig. 5(a)) indicated similar or greater static bed height than plastic particles (Fig. 5(c)) for gas velocities (3–6 m/s) and solids circulation rates ($10.1\text{--}28.3 \text{ kg/m}^2\text{s}$). FCC particles were heavier in density but smaller in size than plastic particles. The effect of particle size seemed to be stronger than particle density.

Fig. 7 shows the comparison of measured static bed height with

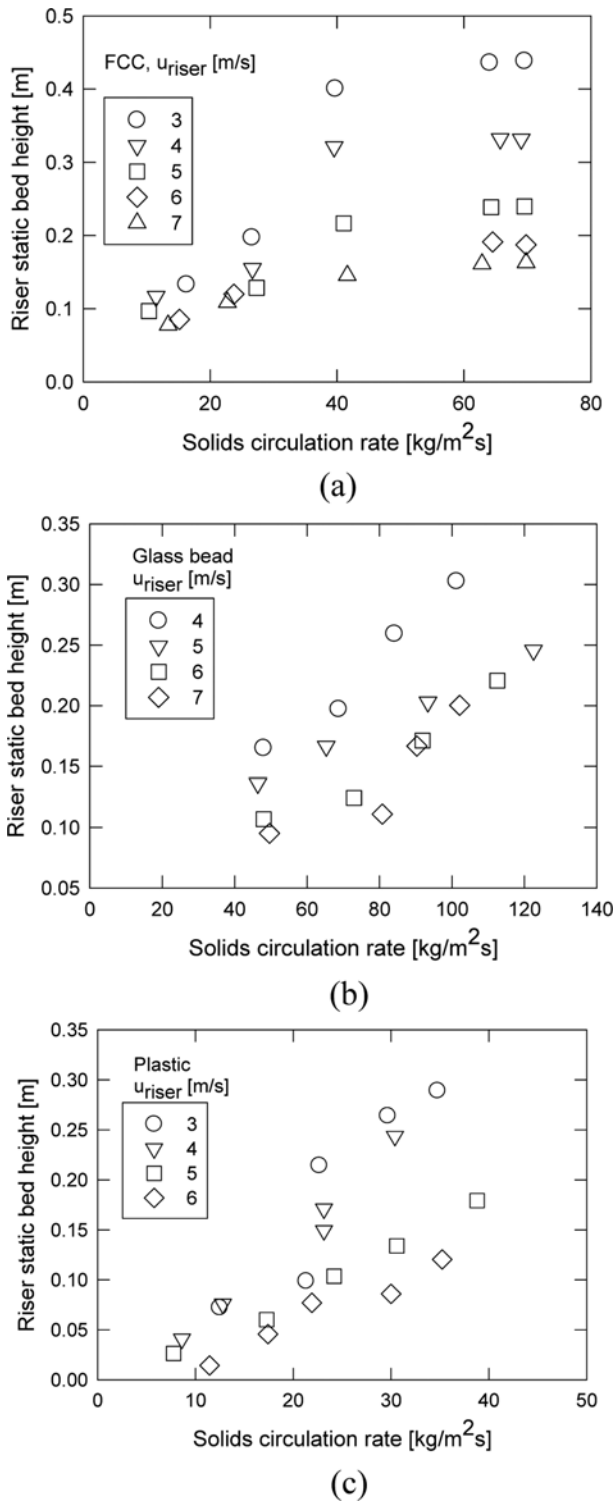


Fig. 5. Effects of gas velocity and solids circulation rate on riser static bed height for (a) FCC, (b) glass bead and (c) plastic powders.

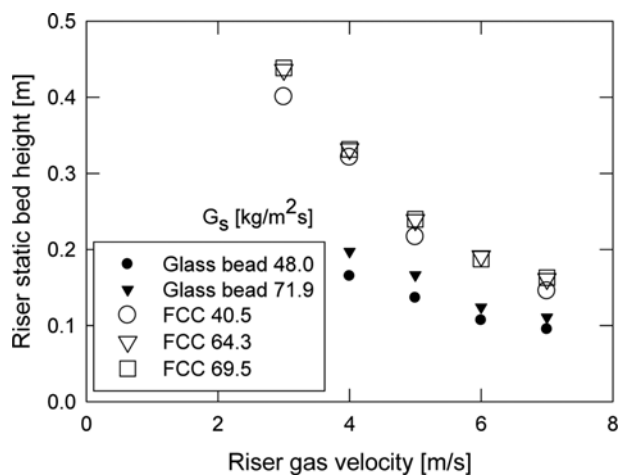


Fig. 6. Comparison of riser static bed height for glass bead and FCC powder.

one calculated by the axial solids holdup profile of Kunii and Levenspiel [11]. Saturation carrying capacity of gas and solids holdups of dense and dilute regions were calculated by correlations of Bai and Kato [4]. The decay factor of the solids holdup profile was calculated by the correlation of Lei and Horio [8] to reflect effects of all variables rather than only the gas velocity effect. The inflection point as height of the dense region was calculated by correlations of Kato et al. [6] and Rao et al. [7] for comparison. Table 2 summarizes the correlations used. As can be seen in the figure, agreement of model calculation was poor. According to the correlation of Bai and Kato [4] on saturation carrying capacity, the dense region only appears at solids circulation rates 64.0 kg/m²s and 69.5 kg/m²s for gas velocity 3 m/s as discussed above. The correlation of Rao et al. [7] (relative deviation (RD)=51.9%, root-mean standard deviation (SD)=0.105 m) seemed to be better than that of Kato et al. [6] (RD=53.6%, SD=0.117 m) overestimating the dense region height considerably. The relative deviation (RD) and the root-mean standard deviation (SD) were calculated by Eqs. (4) and (5), respectively.

$$RD = \frac{100 \sum_{i=1}^N |h_{s,mea} - h_{s,cal}| / h_{s,mea}}{N} \quad (4)$$

$$SD = \sqrt{\frac{\sum_{i=1}^N |h_{s,mea} - h_{s,cal}|^2}{N}} \quad (5)$$

N is the number of data points. The model of Chan et al. [12] was also compared with present data. We followed the calculation procedure given in Table 2 of their study. The model underestimated the static bed height for DF and CAF with AZ (mode II and III, respectively). However, it overestimated for CAF with dense BTFB (mode IV). The residence time of solids in the BTFB was assumed 15 s as in their procedure. The RD and the SD of their model on our data were 196% and 0.583 m, respectively.

Consequently, previous correlations and models on the axial solids holdup profile did not seem to be good enough to apply for estimating the overall solids holdup in the riser. Therefore, we simply correlated the static bed height with experimental variables as follows in SI unit with a correlation coefficient (r^2) 0.832.

$$h_s = 327 \rho_p^{-2.15} d_p^{-0.968} (1 - \epsilon_{mf})^{2.44} G_s^{0.802} u_{riser}^{-1.14} \quad (6)$$

The correlation was applicable in the present experimental ranges: $918 \leq \rho_p$ [kg/m³] ≤ 2486 , $0.0799 \leq d_p$ [mm] ≤ 0.348 , $7.8 \leq G_s$ [kg/m²s] ≤ 122.5 , and $3 \leq u_{riser}$ [m/s] ≤ 7 . Fig. 8(a) depicts comparison of measured static bed height with one calculated by the present correlation (RD=20.5%, SD=0.0370 m). The present simple correlation seemed to be rather more successful than previous correlations. Fig. 8(b) shows a comparison of measured solids circulation flow rate with one calculated by the present correlation (RD=24.4%, SD=10.7 kg/m²s). It reveals the present correlation is feasible to use for estimating the solids circulation rate from riser conditions. However, the correlation still needs to be improved for generalization with more process variables in the future.

CONCLUSIONS

The solids static bed height in the riser increased as the solids

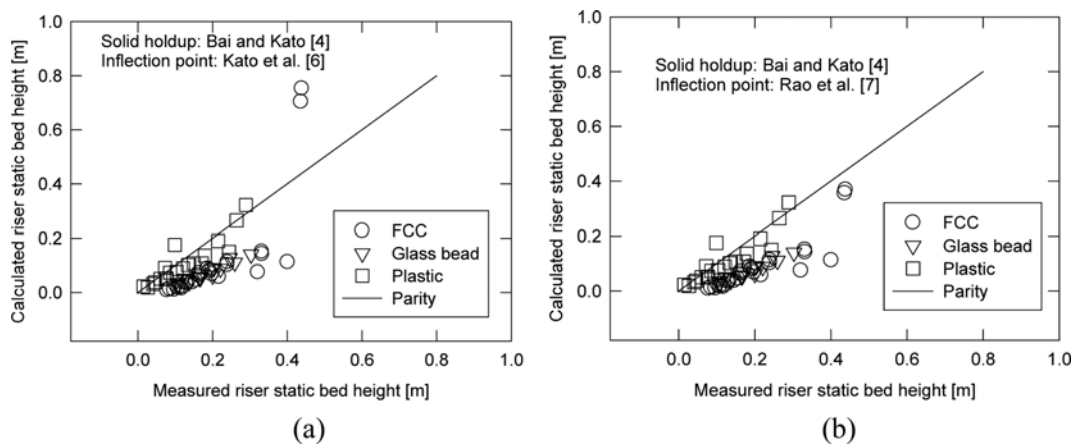
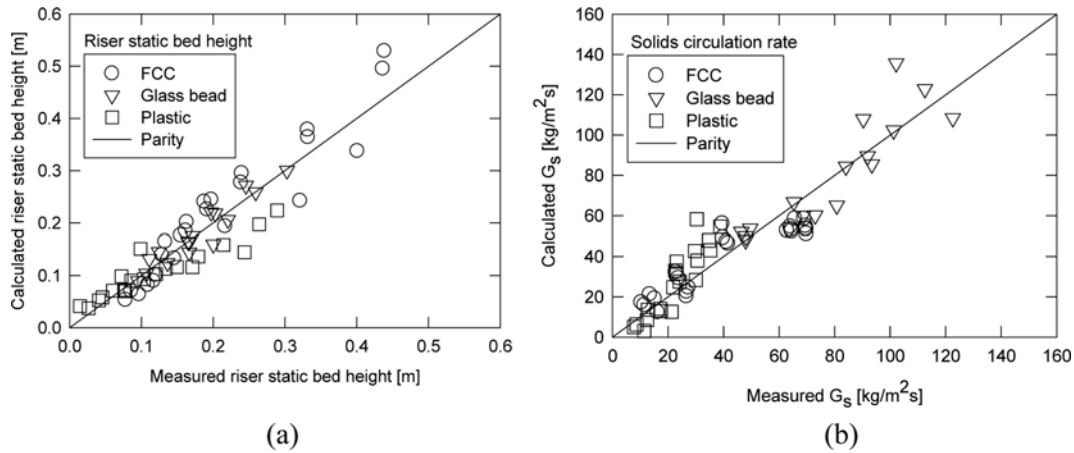


Fig. 7. Comparison of riser static bed height between measured and calculated by the model of Kunii and Levenspiel [11] employing correlations of Bai and Kato [4], Lei and Horio [8], Kato et al. [6], and Rao et al. [7] for model parameters.

Table 2. Correlations on solid holdup, inflection height and decay factor

| Authors | Correlations |
|-------------------|--|
| Bai and Kato [4] | $\frac{\varepsilon_{pd}}{\varepsilon_p} = 1 + 6.14 \times 10^{-3} \left(\frac{u_{riser}}{u_d} \right)^{-0.23} \left(\frac{\rho_p - \rho_g}{\rho_g} \right)^{1.21} \left(\frac{u_{riser}}{\sqrt{gD_r}} \right)^{-0.383} \quad \text{for } G_s < G_s^*$ $\frac{\varepsilon_{pd}}{\varepsilon_p} = 1 + 0.103 \left(\frac{u_{riser}}{u_d} \right)^{1.13} \left(\frac{\rho_p - \rho_g}{\rho_g} \right)^{0.013} \quad \text{for } G_s \geq G_s^*$ $\frac{\varepsilon_p^*}{\varepsilon_p} = 4.04 \varepsilon_p^{0.214} \quad \text{for } G_s < G_s^*$ $\frac{\varepsilon_p^*}{\varepsilon_p} = 1 + 0.208 \left(\frac{u_{riser}}{u_d} \right)^{0.5} \left(\frac{\rho_p - \rho_g}{\rho_g} \right)^{-0.082} \quad \text{for } G_s \geq G_s^*$ $\frac{G_s d_p}{\mu} = 0.125 Fr^{1.85} Ar^{0.63} \left(\frac{\rho_p - \rho_g}{\rho_g} \right)^{-0.44}$ $\varepsilon_p' = \frac{G_s}{\rho_p (u_{riser} - u_t)}$ |
| Kato et al. [6] | $h_t = 360 \left(\frac{G_s}{\rho_p u_t} \right)^{1.2} \left(\frac{u_{riser} - u_t}{u_t} \right)^{-1.45} Re_p^{-0.29}$ |
| Rao et al. [7] | $h_t = 0.180 \left(\frac{G_s}{\rho_p u_t} \right)^{0.205} \left(\frac{u_{riser} - u_t}{u_t} \right)^{-0.325} \left(\frac{d_p}{D_r} \right)^{-0.218} Re_p^{0.1234}$ |
| Lei and Horio [8] | $aD_r = 0.019 \left(\frac{G_s}{u_{riser} \rho_g} \right)^{-0.22} \left(\frac{u_{riser}}{\sqrt{gD_r}} \right)^{-0.32} \left(\frac{\rho_p - \rho_g}{\rho_g} \right)^{0.41}$ |

**Fig. 8. Comparison of measured (a) riser static bed height and (b) solids circulation rate with values calculated by the correlation of this study.**

circulation rate increased; however, it decreased as the gas velocity increased. The effect of gas velocity decreased as the gas velocity increased. The riser static bed height was feasible to use for estimating solids circulation rate with reasonable accuracy. A correlation on static bed height in the riser, relating to the solids circulation rate, was proposed within present experimental ranges, but it has to be improved further in the future because of the low correlation coefficient.

ACKNOWLEDGEMENT

This work was supported by the Energy Efficiency & Resources

of the Korea Institute of Energy Technology Evaluation and Planning (KETEP) grant funded by the Korea government Ministry of Knowledge Economy (2010T100200344).

NOMENCLATURE

- A : cross-sectional area [m²]
- Ar : Archimedes number, $d_p^3 \rho_g g (\rho_p - \rho_g) / \mu^2$ [-]
- a : decay factor [m⁻¹]
- D_r : riser diameter [m]
- d_p : specific surface mean diameter [m]
- Fr : Froude number, $u_{riser} / (gd_p)^{0.5}$ [-]

g : gravitational acceleration, 9.8 [m/s²]
 G_s : solids circulation rate in the riser [kg/m²s]
 G_s^* : saturation carrying capacity of gas [kg/m²s]
 h : height from the distributor [m]
 h_i : h between dense region of particles and dilute region of particles [m]
 h_s : static (or total) bed height of riser solids converted to ε_{mf} condition [m]
 N : number of data [-]
 p : pressure [Pa]
 Re_p : Reynolds number, $d_p u_i \rho_g / \mu$ [-]
 t : time [s]
 r^2 : correlation coefficient [-]
 u_d : superficial solid velocity, G_s / ρ_p [m/s]
 u_{riser} : superficial gas velocity in the riser [m/s]
 u_t : terminal velocity of a single particle [m/s]

Greeks

Δ : difference
 ε_{mf} : voidage at minimum fluidization condition [-]
 ε_p : solid holdup [-]
 ε_p' : solid holdup at uniform flow with slip velocity equal to u_t [-]
 ε_p^* : solid holdup at dilute region [-]
 ε_{pd} : solid holdup at dense region [-]
 μ : gas viscosity [Pa s]
 ρ_g : gas density [kg/m³]
 ρ_p : apparent particle density [kg/m³]
 $\rho_{p,bulk}$: bulk particle density [kg/m³]

Subscripts

b2 : bubbling fluidized bed (2)
 cal : calculated
 mea : measured

r : riser

REFERENCES

1. J.-H. Choi, C.-K. Yi and S.-H. Jo, *Korean J. Chem. Eng.*, **28**, 1144 (2011).
2. J.-H. Choi, C.-K. Yi, S.-H. Jo and H.-J. Ryu, *Adv. Powder Technol.*, **22**, 657 (2011).
3. L. de Martin and J. R. van Ommen, *Chem. Eng. J.*, **204-206**, 125 (2012).
4. D. Bai and K. Kato, *Powder Technol.*, **101**, 183 (1999).
5. J.-H. Choi, C.-K. Yi and J. E. Son, *Korean J. Chem. Eng.*, **7**, 306 (1990).
6. K. Kato, H. Shibasaki, K. Tamura, S. Arita, C. Wang and T. Takarada, *J. Chem. Eng. Jpn.*, **22**, 130 (1989).
7. V. V. B. Rao, R. K. Saha and P. S. Gupta, *Indian Chemical Engineer, Section A, J. of Indian Institute of Chemical Engineers*, **38**, 91 (1996).
8. H. Lei and M. Horio, *J. Chem. Eng. Jpn.*, **31**, 83 (1998).
9. Y. Li and M. Kwauk, in *Fluidization*, J. R. Grace and J. M. Matsen Eds., Plenum Press, New York (1980).
10. T. M. Knowlton, in *Circulating fluidized beds*, J. R. Grace, A. A. Avidan and T. M. Knowlton Eds., Blackie Academic & Professional, Chapman & Hall, New York (1997).
11. D. Kunii and O. Levenspiel, *Fluidization engineering*, 2nd Ed., Butterworth-Heinemann, Boston (1991).
12. C. W. Chan, J. P. K. Seville, D. J. Parker and J. Baeyens, *Powder Technol.*, **203**, 187 (2010).
13. H. T. Bi and J. R. Grace, *Int. J. Multiphase Flow*, **21**, 1229 (1995).
14. D. Geldart, *Powder Technol.*, **7**, 285 (1973).
15. U. Arena, A. Cammarota and L. Pistone, in *Circulating fluidized bed technology*, P. Basu Eds., Pergamon Press, New York (1985).
16. M. Louge and H. Chang, *Powder Technol.*, **60**, 197 (1990).
17. C. M. H. Brereton and J. R. Grace, in *Circulating fluidized bed technology IV*, A. A. Avidan Eds., AIChE (1994).